

Review

Recent Computational Advances Regarding Amyloid- β and Tau Membrane Interactions in Alzheimer's Disease

Phuong H. Nguyen¹ and Philippe Derreumaux^{1,2,*}

¹ CNRS, Laboratoire de Biochimie Théorique, Institut de Biologie Physico-Chimique, Fondation Edmond de Rothschild, Université Paris Cité, UPR 9080, 13 rue Pierre et Marie Curie, 75005 Paris, France; phuong.nguyen@ibpc.fr

² Institut Universitaire de France (IUF), 75005 Paris, France

* Correspondence: philippe.derreumaux@ibpc.fr

Abstract: The interactions of amyloid proteins with membranes have been subject to many experimental and computational studies, as these interactions contribute in part to neurodegenerative diseases. In this review, we report on recent simulations that have focused on the adsorption and insertion modes of amyloid- β and tau proteins in membranes. The atomistic-resolution characterization of the conformational changes of these amyloid proteins upon lipid cell membrane and free lipid interactions is of interest to rationally design drugs targeting transient oligomers in Alzheimer's disease.

Keywords: amyloid; aggregation; simulations; Alzheimer's disease; membrane

1. Introduction

Amyloid- β (A β) proteins of residues 40 and 42 and tau isoforms of residues 352–421, which are linked to Alzheimer's disease (AD), have the propensity to aggregate into amyloid fibrils with a cross- β structure [1,2] and multiple polymorphs, as observed by Scheres et al. and Tycko et al. [3,4]. Aggregation proceeds through primary and secondary (surface catalysis and fragmentation) nucleation mechanisms, fibril growth, and depolymerization in various experimental conditions [5].

The A β 42 sequence consists of hydrophilic, charged, N-terminal residues 1–16; the central hydrophobic core (CHC, residues 17–21); a hydrophilic region (residues 22–28) and hydrophobic residues 30–42. Numerous studies have reported that low-molecular-weight (LMW) oligomers of A β generated during the lag phase of aggregation or released from the fibrils are the key players in AD [1,6,7]. The aggregation kinetics of A β 42 in aqueous solution has been continuously studied to understand the impact of pH variation [8], N-terminal residues [9], and mixing with C-terminal truncated species such as A β 24 [10]. The computational structure characterization of A β 42 and tau monomer/dimer in aqueous solution has been pursued [11–15].

Tau oligomers are toxic in vitro, seeding the propagation of AD pathology [16], and the tau 297–391 fragments form fibrils under physiological conditions similar to those found in AD brain tissues [17]. Single immunogold-labeled transmission electron microscope (TEM) and fluorescence spectroscopy revealed the presence of a tyrosine–tyrosine crosslink at position 310 on AD-brain-derived tau oligomers and fibrils [18].

The etiology of AD is linked in part to the mediated effects of A β and tau on neuronal cell membranes. Atomic force spectroscopy (AFM) revealed that the self-assembly of A β was enhanced and occurred at nanomolecular concentrations on two lipid bilayers formed by 1-palmitoyl-2-oleoyl-glycero-3-phosphocholine (POPC, PC) and 1-palmitoyl-2-oleoyl-sn-glycero-3-phospho-l-serine (POPS, PS) [19]. The presence of cholesterol in the membrane enhanced the primary nucleation of A β 42 by several orders of magnitude compared with that in aqueous solution, as assessed using thioflavin T (ThT) fluorescence [20]. The experimental techniques used to study the amyloid–membrane interactions through the



Citation: Nguyen, P.H.; Derreumaux, P. Recent Computational Advances Regarding Amyloid- β and Tau Membrane Interactions in Alzheimer's Disease. *Molecules* **2023**, *28*, 7080. <https://doi.org/10.3390/molecules28207080>

Academic Editor: Tigran Chalikian

Received: 5 September 2023

Revised: 26 September 2023

Accepted: 12 October 2023

Published: 13 October 2023



Copyright: © 2023 by the authors. Licensee MDPI, Basel, Switzerland. This article is an open access article distributed under the terms and conditions of the Creative Commons Attribution (CC BY) license (<https://creativecommons.org/licenses/by/4.0/>).

carpeting, detergent-like removal of lipids, and amyloid-pore hypotheses and to study experimental imaging A β membrane interactions were recently reviewed [21,22].

Structures of A β -membrane assemblies are challenging experimentally as they are metastable and heterogeneous. Among the new experimental results, using mass spectrometry and nuclear magnetic resonance (NMR) spectroscopy in dodecylphosphocholine (DPC) micelles, Carulla et al., at pH 9.0, provided the high-resolution structure of the A β 42 tetramer and octamer, revealing conductivity pores as a mechanism for the damage of the membrane. The tetramer conformation comprises a six-stranded β -sheet core with the two external A β peptides forming β hairpins (Figure 1) [23]. Cryoelectron tomography was used to obtain 3D nanoscale images of the interactions of various A β assemblies with liposomes. A β oligomers and protofibrils bind to the vesicles, and insert and carpet the upper leaflet of the bilayer, allowing oligomers to establish a network of A β linked to liposomes. The monomeric and fibrillar A β species have almost no impact on the membrane [24]. It was also evidenced that the A β oligomers generated during secondary surface nucleation disrupt membrane integrity, and time-resolved fluorescence microscopy of individual synthetic vesicles demonstrated that the disruption of lipid bilayers correlates with the levels of secondary nucleation-generated A β 42 oligomers [25]. Experiments also showed that ganglioside-enriched vesicles promoted A β oligomerization and disruption of the membrane [26]. The impact of metal ions or lipid vesicles on A β aggregation has been studied [2,27,28]; their combined effects are not well understood. It was shown, however, that the co-effect of Cu $^{2+}$ and lipid vesicles led to the rapid formation of abundant A β 40 LMW oligomers containing β -sheet-rich structures [29].

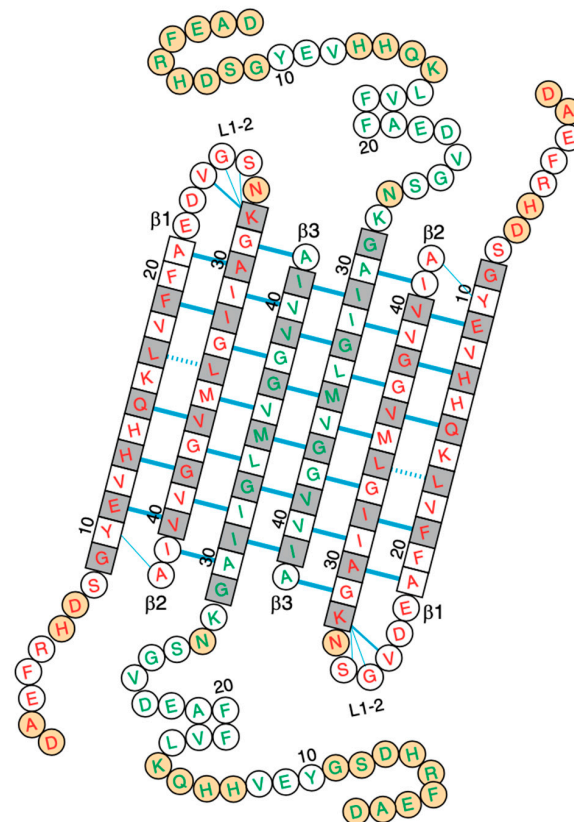


Figure 1. Experimentally derived conformation of the A β 42 tetramer in a membrane model with a six-stranded β -sheet core and the two external A β peptides forming β hairpins, as proposed in Ref. [23].

Surface-enhanced infrared (IR) absorption spectroscopy and atomic force microscopy (AFM) were used to study the structural morphology of A β 42 aggregation on distinct two-dimensional self-assembled monolayers (SAMs). On hydrophobic interfaces, the

interactions with the C terminus of A β 42 promote the formation of small oligomers with low contents of β -sheet structures. On hydrophilic interfaces, H-bond and electrostatic interactions result in the promotion of large oligomers with a β -sheet structure [30]. Solid-state NMR (ss-NMR) was used to investigate the interactions between A β 40 peptides and synaptic plasma membranes extracted from rat brain tissues. It was found that, at the membrane-associated nucleation stage, the G25-V36 residues initialized the assembling of low-order β -sheet structures, and the F19-G25 residues were closely linked with lipids [31]. Using high speed AFM and nanoscale infrared spectroscopy (IR) on A β 42 L34T and G37C variants with a POPC/sphingomyelin (SM)/cholesterol/monosialotetrahexosyl-ganglioside (GM1) membrane, Molinari et al. showed that membrane disruption was associated to small oligomers with an antiparallel β -sheet structure [32]. It is worth noting that nonequilibrium flowing conditions promote the aggregation of A β on 1,2-dimyristoyl-sn-glycero-3-phosphocholine (DMPC) bilayers [33].

Various studies have reported the presence of both extracellular and intracellular A β assemblies. Using large unilamellar vesicles to model different locations of membranes, including the inner leaflet (IL) and outer leaflet (OL) of the plasma membrane, late endosomes, the endoplasmic reticulum (ER), and the Golgi apparatus, A β 42 aggregation was monitored using fibril mass concentration as a function of time. A β 42 aggregation enhancement was observed in IL, OL, and late endosomes. The membrane in the inner leaflet consisted of 22% PC, 40% PE, 26% PS, and 12% cholesterol (chol); the membrane in the outer leaflet consisted of 30% PC, 5% PS, 35% SM and 30% chol; and the membrane in late endosomes consisted of 40% PC, 15% PE, 7% SM, 23% chol, and 11% bis(monoacylglycerol)phosphate (BMP). A β 42 aggregation inhibition was observed in the Golgi membrane, consisting of 43% PC, 17% phosphatidylethanolamine (PE), 9% phosphatidylinositol (PI), 17% SM, and 14% chol; and in the ER membrane, consisting of 52% PC, 26% PE, 9% PI, and 13% chol [34].

In comparison with A β , the number of experimental studies on LMW tau oligomers-membranes is fairly small. It is known that tau oligomers interact with the plasma membrane via multiple binding modes with the N-terminal projection domain (residues 1–243 containing a proline-rich region), and the R1–R4 repeats (residues 244–369) [1,35]. Tau interacts with phospholipid tails, facilitating the formation of stable protein–lipid complexes, facilitating cell-to-cell transport [36]. Like A β oligomers, tau oligomers can remodel and disrupt membranes, extract lipids, and form pores, and these effects are modulated by protein concentrations and lipid compositions [37–39].

The aim of this review is to report on recent computational studies starting the year 2020, aimed at understanding the effects of A β 40 and A β 42 alloforms and long tau isoforms on and in cell membranes and vice versa, and the interactions between free lipids and A β peptides.

2. Adsorption and Insertion of Amyloid- β

Determining the structures of A β -membrane assemblies is a computational challenge. The interaction of an A β monomer with membranes was investigated via a series of simulations. Using a CHARMM36m force field and molecular dynamics (MD) simulation, Strodel et al. showed the partial insertion of an A β 42/POPC complex into a 1,2-dioleoyl-sn-glycero-3-phosphocholine (DOPC) bilayer and a deeper insertion of parts of A β 42 compared with a single peptide [40]. Alonso et al. investigated the interactions of A β 42 monomers with lipid bilayers consisting of POPC and small amounts (1–5 mol%) of GM1. Using MD simulations with the GROMOS force field, isothermal calorimetry, and Langmuir balance experiments, they showed that A β 42 adsorbs, and cannot insert into, GM1-containing phospholipid membranes in the liquid-disordered (Ld) state. They also found that GM1, up to 3 mol%, increased A β 42 binding to the bilayer [41]. Using the same experimental techniques and a membrane consisting of 47.5% POPC, 47.5% SM, and 5% GM1, they found that A β 42 monomer, but also oligomers and to a lesser extent fibril preparations, inserted into membranes in the liquid-ordered (Lo) state [42].

Hamiltonian replica exchange molecular dynamics simulations with the OPLS force field were performed to determine the impact of oxidized (ox) G25, G29, and G33 residues on monomeric A β 42 interacting with a membrane made of 70% POPC, 25% cholesterol, and 5% GM1. Owen et al. found that A β 42 wild-type (WT) and A β 42-oxG25 peptides have a lower tendency to bind to GM1 than A β 42-oxG29 and A β 42-oxG33, and the WT monomer has a higher propensity to insert into the membrane than the three oxidized alloforms [43]. A 2.5 μ s MD simulation of A β 42-Cu²⁺ with a DMPC bilayer revealed that the presence of calcium ions mediated membrane perturbation and inhibited the penetration of the A β 42 monomer into the membrane [44]. Interestingly, the decrease in the bending rigidity of the POPC membrane, as a result of the incorporation of A β 40 and A β 42 monomers, was observed using MD studies and experimental flicker-noise techniques [45]. Finally, Localito et al. studied the interaction of monomeric alpha-helical A β 40 (WT, H13P, H14P, L17P, and F20P) using three replicates with a single DEPC lipid. From their simulations, they hypothesized that the alpha-helix is a fundamental requirement to fulfill the lipid-chaperon model [46].

The dynamics of A β dimers at the surface or inserted into multiple membrane models were also explored. Chang et al. used atomistic Brownian dynamics simulations to study the association of two A β 42 monomers on SAM surfaces. The conformations included the fibril-like β -rich structure and a random coil structure with a low alpha-helix content. Four SAM surfaces were used, including undecanethiol (hydrophobic, referred to as CH₃-SAM), 11-mercapto-1-undecanol (hydrophilic, OH-SAM), 11-amino-1-undecanethiol (cationic, NH⁺-SAM), and 11-mercaptoundecanoic acid (anionic, COO⁻-SAM) on a gold substrate. Monomers started to diffuse from a random position at a height of 40 nm above the SAM surfaces. A total of 1000 trajectories for each rigid-body protein conformation was performed to calculate the association and residence times on the four SAM surfaces. For three SAM surfaces, the exception being NH⁺-SAM, the averaged monomer–dimer association time was in the order of 9–10 μ s for the β -rich conformation and 5 μ s for the random coil conformation, indicating a 5–35% decrease in association time due to the presence of a surface. The residence time was found to vary from 7.4 (OH-SAM) to 8.8 (CH₃-SAM) μ s. The monomer–dimer association time on NH⁺-SAM with heterogeneous charge distribution could not be assessed as the monomers were not able to associate, because they were strongly bound to the SAM. The addition of Na⁺ greatly enhanced the diffusion on the COO⁻-SAM. This finding emphasizes the importance of considering the role of Na⁺ in vitro [47].

In a second μ s MD simulation, Lyubchenko et al. examined the formation of the A β 42 dimer modeled using the ff99sb-ildn force field with a POPC bilayer. They revealed a β -sheet content of 10% and an alpha-helix content fluctuating between 10 and 35%, with the N-terminal residues and residues 29–31 having the highest propensity to interact. Of interest is that the on-surface aggregation process is dynamic, and oligomers assembled on the surface can dissociate into the solution. These results suggest that on-surface aggregation is one mechanism through which A β 42 oligomeric species in solution are produced [19].

In a third μ s MD simulation, Strodel et al. compared A β 42 dimerization, modeled using the CHARMM36m force field, in aqueous solution and at a lipid bilayer surface mimicking a neuronal membrane composed of 38% PC, 24% PE, 5% PS, 20% chol, 9% SM, and 4% GM1. They found that the neuronal membrane reduces the dynamics of membrane-bound A β 42 and inhibits β -sheet formation (β -sheet content of 28%) due to the hydrogen bonds with the sugar groups of GM1. This result is in contrast to the dimerization in the aqueous phase characterized by a random coil to β -sheet transition, which leads to a β -sheet content of 36%, similar to the content observed in A β fibrils. The insertion of the peptides into the hydrophobic region of the membrane was not observed, and the membrane was marginally affected [48].

In a fourth study, Fazli et al. performed three MD simulations of 200 ns each at three temperatures with the OPLS force field for proteins to explore the early interaction steps of

two separated parallel A β 40 peptides with the helix-structure content spanning residues 15–37 partially inserted into a DPPC bilayer. Upon association, the helical region becomes disrupted to two smaller fragments with a kink, and the dimeric A β species has two types of distribution in DPPC at 300, 310 and 330 K. In the first distribution, the two peptides remain embedded in top leaflet, while in the second distribution, at least one of the peptides penetrates into the bottom leaflet, leading to the local disordering of the DPPC bilayer [49].

Guo and Wang used atomistic MD simulations for a total of 48 μ s to investigate the effects of cholesterol on A β 42 dimerization in lipid DOPC bilayers with different molar ratios of cholesterol (0, 20, and 40 mol %). Cholesterol reduces the time for the formation of stable dimers and has two effects on A β –membrane interactions. Firstly, cholesterol enhances the extraction of the C-terminal region from the membrane to the bulk solution. At the ratios of 0 and 20 mol %, A β dimers are attached at the membrane–water interface, and at a ratio of 40 mol %, they are repelled to water. Secondly, cholesterol reduces A β –membrane interactions, thereby augmenting dimeric interactions [50].

Other coarse-grained (CG) 120 μ s MD simulations, performed by Parisini et al., demonstrated the interactions between trimeric or hexameric A β 40 fibrils with a 100% DPPC bilayer, a 70% DPPC–30% chol bilayer, or a 50% DPPC–50% chol bilayer. The spontaneous binding of the A β 40 fibrils to the membranes was captured with the CHC (residues 17–21), the K16 residue, and the C-terminal hydrophobic residues involved in the process. Moreover, they showed that while the A β 40 fibril does not bind to the 100% DPPC bilayer, its binding affinity to the membrane increases with the amount of cholesterol [51].

Coarse-grained Martini MD simulations, performed by Cheng et al., revealed the binding of A β 17–42 fibrillar dimers–pentamers to interfacial liquid-ordered (Lo) and liquid-disordered (Ld) regions in phase separated lipid rafts with distinct membrane-bound conformations [52]. CG Martini simulations of several μ s, generated by Cruz et al., showed the role of cholesterol in the binding of A β 11–42 and A β 17–42 fibrils to lipid bilayers containing 30 and 50% cholesterol by promoting electrostatic interactions [53]. By using atomistic MD simulations, A β 12 mers were found to more disrupt a neuronal membrane than a fibril [54], with the peptide and membrane parameterized by the CHARMM36m and CHARMM36 force fields, respectively.

3. Detergent Effect of Amyloid- β

Amyloid- β oligomers have a strong detergent effect on lipid bilayers [2]. Cholesterol, a component of membranes, is a risk factor in AD, being present in AD senile plaques with a molar ratio of 1:1 [55], and its level in the brain correlating with the severity of dementia in AD individuals [56].

Nguyen and Derreumaux performed atomistic replica exchange molecular dynamics and replica exchange with solute tempering on the dimer/trimer of A β 42 with cholesterol at a ratio 1:1 [57,58]. They found that the binding spots of cholesterol essentially involve the CHC and L30–M35 residues. The contribution of D22–K28 and the N-terminus residues was also detected. Cholesterol is rarely inserted into the aggregates. Rather, cholesterol molecules are attached as dimers and trimers at the surface of A β 42 trimers, proposing that they act as a glue to promote the formation of larger aggregates. The formation of larger A β 42 aggregates due to the presence of free cholesterol was confirmed using AFM images of A β 42/cholesterol on a lipid bilayer, and it was shown that these aggregates can accumulate in the bulk solution [59].

The impact of free GM1, abundant in mammalian brains, on the two A β isoforms was investigated in a combined NMR-MD study performed by Brooks et al. This study revealed the formation of well-ordered, structurally compact GM1+A β complexes, altering A β aggregation [60]. The presence of free fatty acids such as lauric acid was found computationally by Hansmann et al. to stabilize ring-like and barrel-shaped A β 42 oligomers [61]. Similar to the simulation results of A β 42/cholesterol, simulations of the A β 42 monomer with 1,2-dimyristoyl-sn-glycero-3-phosphocholine (DMPC) provided evidence that the unfolded A β 42 peptide adheres to the lipid cluster rather than embeds into it [62]. MD sim-

ulations on the μs time scale revealed that three free POPC lipids trigger a disorder-order (α -helix, β -strand) transition in the $\text{A}\beta_{42}$ monomer [48].

4. Amyloid- β Pore Formation

Membrane-embedded $\text{A}\beta$ species with membrane conductance, which do not display a ThT fluorescence signal, can have a wide range of conformations and oligomer sizes [2]. Some form well-defined pores [63–65] made, for instance, of six-stranded β -sheet and β -sandwich structures (Figure 1), and other species are spherical without any evidence of discrete channel or pore formation. Atomistic MD simulations showed that many concentric β barrels are consistent with image-averaged electron micrographs [66,67], revealing the strong role of $\text{A}\beta$ β -sheet edge conformations in the permeabilization of the membrane [68]. Interestingly, using MD simulations, quantum mechanics, and experimental techniques, La Rosa et al. showed that $\text{A}\beta_{40}$ can also form α -helix channels through the GxxG motif [69].

In a recent study, the dynamics of an S-shaped $\text{A}\beta_{42}$ cross- β hexamer model inserted into a lipid bilayer membrane were explored by Nguyen and Derreumaux using two atomistic MD simulations, each two microseconds long [70]. The initial model was characterized by the CHC and residues 30–42 embedded into a DOPC bilayer membrane (Figure 2). Structural secondary, tertiary, and quaternary rearrangements were observed, leading to two distinct metastable species, hexamer and two trimers, accompanied by membrane disruption and water permeation. The study provides evidence of hexamers and trimers with the N-terminal residues located in the top and bottom leaflets of the membrane and a minimal lifetime of several microseconds. Some conformations, but not the majority, have the CHC and C-terminal hydrophobic residues exposed to the solvent. The MD simulations also showed that residues 1–10 in both trimers of run 1, in trimer 1 of run 2, and residues 1–16 in trimer 2 of run 2 were exposed to the solvent (Figure 3). This result is consistent with many simulations of $\text{A}\beta_{42}$ oligomers partially embedded in the membrane [2]. We did not find evidence of β hairpins in the N terminus, as reported for $\text{A}\beta_{42}$ dimers in DOPC bilayers [71]. Overall, the high solvent accessibility of residues 1–16 may help with understanding the linking of liposomes through $\text{A}\beta$ oligomers, as assessed via cryoelectron tomography [22].

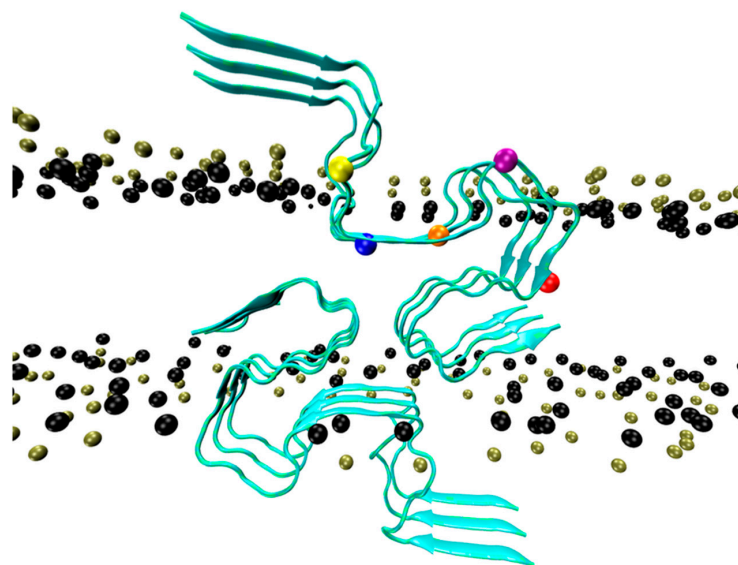


Figure 2. Initial conformation of the $\text{A}\beta_{42}$ hexamer. View in the x direction, parallel to the fibril axis. We show the ribbon structure of the hexamer, the phosphate atoms (tan), and the O21 and O22 atoms of the glycerol (black). Also shown are the $\text{C}\alpha$ atom of V12 (yellow), Q15 (blue), V18 (orange), E22 (purple), and K28 (red) [70].

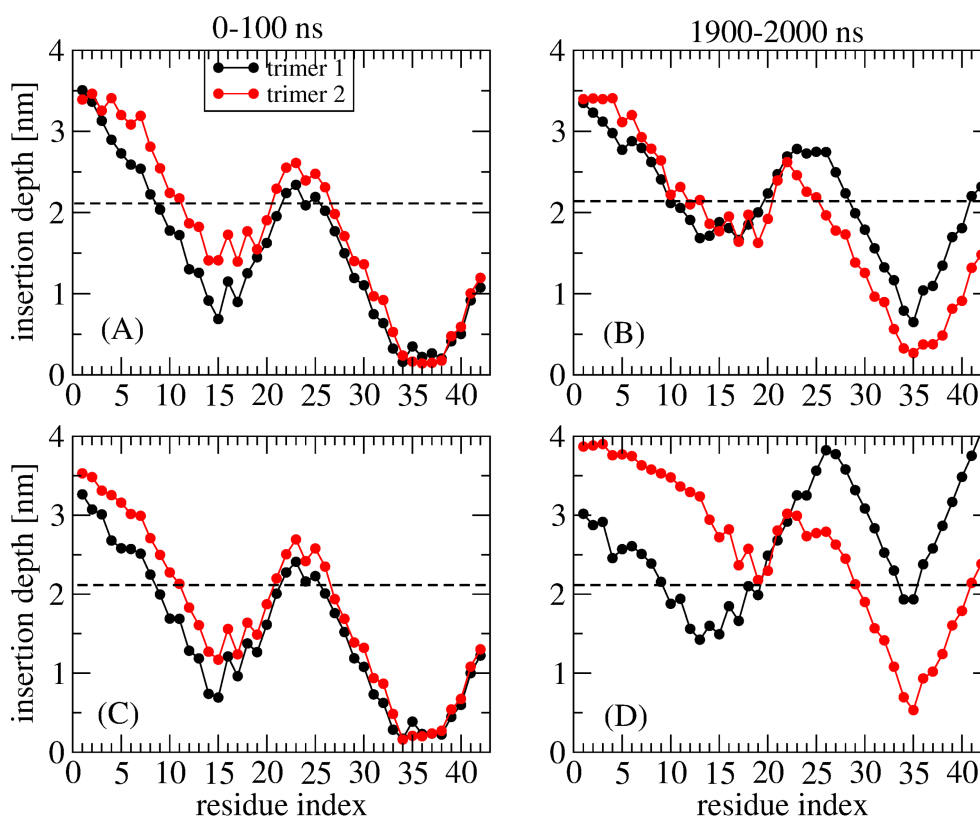


Figure 3. MD-generated insertion depths of the residues belonging to trimer 1 and trimer 2 in two time intervals: 0–100 ns and 1900–2000 ns. (A,B) MD run 1 at 303 K and (C,D) MD run 2 at 310 K [70]. The three chains in aqueous solution at the upper leaflet of the membrane are referred to as trimer 1 and the other three chains at the lower leaflet of the membrane are referred to as trimer 2.

5. Tau–Membrane Interactions

Zhou et al. reported the computational results of the tau K19 (R1, R3, and R4) monomer bound to a POPC/POPS membrane using the ff14SB force field for proteins [72]. Based on previous electron paramagnetic resonance (EPR) results, which established the presence of one helix in each repeat [73], their biased MD simulations on the microsecond timescale showed that the three amphipathic helices stably bind to a POPC–POPS membrane and revealed an important difference in membrane binding stability between the repeats R1 and R3 and R4. In each amphipathic helix, however, a lysine conserved among the microtubule-binding regions, along with other charged and polar sidechains, interacts with lipid headgroups. Furthermore, a conserved valine along with two other nonpolar sidechains insert into the hydrophobic region of the membrane. These two conserved residues form similar interactions with microtubules as observed from the cryo-EM microtubule-bound structure of tau 202–395 [74]. Zhou et al. proposed that this partial mimicry facilitates the transfer of tau from membranes to microtubules [72].

Nguyen and Derreumaux performed MD simulations of the tau R3–R4 domain monomer at the surface of a DOPC–DOPS lipid bilayer, with residues 306–378 forming the fibril core of full-length tau alloforms in the brain of individuals with AD [75]. The two simulations showed that the surface of the membrane does not induce β -sheet formation and leads to an ensemble of structures very different from those in the bulk solution. They also revealed the dynamic interactions of the membrane-bound state of the tau R3–R4 monomer, allowing insertion of the PHF6 motif (residues 306–311), and residues 312–318 and 376–378.

As tau dimers are observed in cells and in the cerebrospinal fluid of AD patients [76], Nguyen and Derreumaux performed MD simulations on the tau R3–R4 domain dimer starting from a cryo-EM state and a compact globular state (Figure 4). They found distinct

insertion depths depending on the initial conformation and transient adsorption of the PHF6 motif on the membrane as the results of the high propensity of PHF6 to form parallel β -sheets, and insertion of the C-terminal R4 region into the membrane (Figure 5) [77]. There are therefore differences between the monomer and dimer results. To what extent the dimer results can be extrapolated to full-length tau remains to be determined, as the R2 repeat interacts with negatively charged vesicles [38].

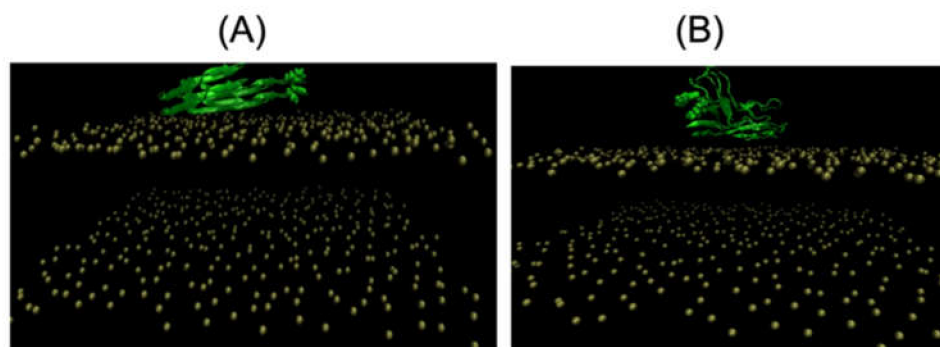


Figure 4. The two initial tau 306–378 dimer conformations. In both panels, the phosphate atoms of the lipid heads are in tan, and we show the van der Waals representation of the side chains of F378 residue in green. (A) Initial cryo-EM state. (B) Initial globular compact state [77].

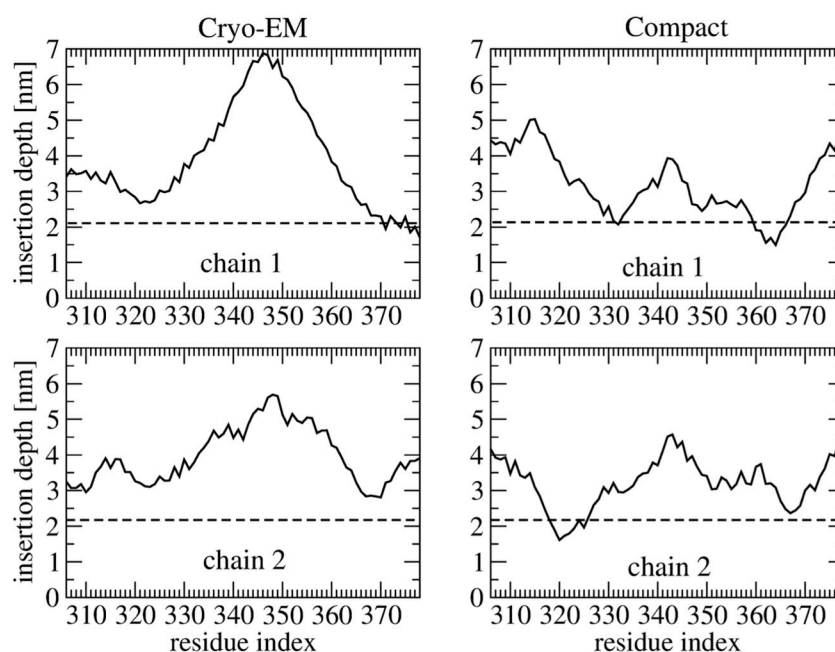


Figure 5. Average insertion depth of each residue of the two tau 306–378 chains using 1950–2000 ns of the MD simulation starting from the cryo-EM structure (left) and the globular compact structure (right) [77].

Using 15 μ s coarse-grained Martini MD simulations followed by all-atom (AMBER99sb and Slipid force fields) 200 ns MD simulations with the residues spanning the R2-R3 domain initially adopting the fibril cryo-EM conformation, the transient interactions of tau K18 (containing the four repeats) oligomers (dimer and tetramer) on three lipid rafts (control raft, modified CO-raft containing GM1 clusters on one leaflet (GM-raft), and modified CO-raft containing PS clusters on one leaflet (PS-raft)) were investigated. Their raft systems included DPPC, DLPC, and cholesterol in all cases. It was found that tau K18 prefers to bind to the boundary domains (Lod) created by the coexisting Lo and Ld domains in the

lipid rafts. The stronger binding of tau K18 oligomers to the GM1 and phosphatidylserine (PS) domains was reported, and K18-induced lipid chain order disruption and tau K18 β -sheet formation were detected. The results suggest that GM1 and PS domains, located in the outer and inner leaflets of the neuronal membranes, respectively, are specific membrane domain targets of tau oligomers, and the Lod domains are not. Clearly, much longer all-atom MD simulations are required to identify more stable β -sheet structures on the raft surfaces [78].

Finally, the interactions of tau fibrils with membrane lipids were studied via a multi-scale simulation. Based on the CG Martini protocol followed by all-atom CHARMM36 force field 400 ns MD simulations, Bargava et al. studied the interactions of R3-R4 tau filament consisting of two protofibrils with 14 membrane systems consisting of POPC, 1-palmitoyl-2-oleoyl-sn-glycero-3-phosphatidylethanolamine (POPE), 1-palmitoyl-2-oleoyl-sn-glycero-3-phosphatidyl-glycerol (POPG) along with cholesterol for seven different compositions. Tau proteins do not interact similarly with the zwitterionic lipid membranes compared with the charged lipid membranes, with the negatively charged POPG membranes enhancing the binding propensity of tau fibrils. Cholesterol addition alters tau binding affinity with the membrane. The binding of tau fibril induces the loss of the β sheet of the tau residues, destabilizes β -sheet regions depending on the lipid composition and the percentage of cholesterol concentration, and changes the membrane properties including thickness and order parameters of the tails [79].

6. Conclusions

We focused on recent simulations, aimed at understanding the adsorption and insertion modes of the two main amyloid proteins associated with AD in various membrane models. Our experimental and computational knowledge on the aggregation and structures of tau isoforms is increasing at a much slower pace than that of A β .

Major challenges were identified in the field. For instance, new experimental methods of biomolecular processes in membranes, spanning the microsecond time resolution and detecting populations of intermediates below the percent range, would be very useful for validating the MD-generated models. The impact of fluid flow on lipid bilayers–amyloid protein interactions should also be investigated both experimentally and computationally, as it is known that cells have extracellular matrices that may have very different behaviors compared to vesicles and planar lipid bilayers in the absence of membrane protein receptors.

Most simulations have started from the alpha-helical and fibrillar states, so repeating the simulations with antiparallel orientations of the peptides and longer timescales would provide more information on the conformational ensemble and its impacts on the membrane. The results of recent computations showed that free lipids (cholesterol, GM1) and fatty acids alter the energy landscape of A β 42 species, and cholesterol induces the formation of much larger A β 42 aggregates, which might generate species more difficult to clean from the brain's interstitial system. More information on the large gap between simulations and in vivo conditions can be found in Ref. [15].

Author Contributions: Conceptualization, P.H.N. and P.D.; writing—original draft preparation, both authors; writing—review and editing, both authors. All authors have read and agreed to the published version of the manuscript.

Funding: This research received no external funding.

Institutional Review Board Statement: Not relevant.

Informed Consent Statement: Not applicable.

Data Availability Statement: Not applicable as this is a review article.

Acknowledgments: We acknowledge support the “Initiative d’Excellence” program from the French State, Grant “DYNAMO”, ANR-11-LABX-0011.

Conflicts of Interest: The authors declare no conflict of interest. The funders had no role in the design of the study; in the collection, analyses, or interpretation of data; in the writing of the manuscript; or in the decision to publish the results.

References

1. Nasica-Labouze, J.; Nguyen, P.H.; Sterpone, F.; Berthoumieu, O.; Buchete, N.V.; Coté, S.; De Simone, A.; Doig, A.J.; Faller, P.; Garcia, A.; et al. Amyloid β Protein and Alzheimer's Disease: When computer simulations complement experimental studies. *Chem. Rev.* **2015**, *115*, 3518–3563. [[CrossRef](#)] [[PubMed](#)]
2. Nguyen, P.H.; Ramamoorthy, A.; Sahoo, B.R.; Zheng, J.; Faller, P.; Straub, J.E.; Dominguez, L.; Shea, J.E.; Dokholyan, N.V.; De Simone, A.; et al. Amyloid oligomers: A joint experimental/computational perspective on Alzheimer's disease, Parkinson's disease, type II diabetes, and amyotrophic lateral sclerosis. *Chem. Rev.* **2021**, *121*, 2545–2647. [[CrossRef](#)] [[PubMed](#)]
3. Shi, Y.; Zhang, W.; Yang, Y.; Murzin, A.G.; Falcon, B.; Kotecha, A.; van Beers, M.; Tarutani, A.; Kametani, F.; Garringer, H.J.; et al. Structure-based classification of tauopathies. *Nature* **2021**, *598*, 359–363. [[CrossRef](#)] [[PubMed](#)]
4. Lee, M.; Yau, W.M.; Louis, J.M.; Tycko, R. Structures of brain-derived 42-residue amyloid- β fibril polymorphs with unusual molecular conformations and intermolecular interactions. *Proc. Natl. Acad. Sci. USA* **2023**, *120*, e2218831120. [[CrossRef](#)] [[PubMed](#)]
5. Michaels, T.C.T.; Šarić, A.; Curk, S.; Bernfur, K.; Arosio, P.; Meisl, G.; Dear, A.J.; Cohen, S.I.A.; Dobson, C.M.; Vendruscolo, M.; et al. Dynamics of oligomer populations formed during the aggregation of Alzheimer's A β 42 peptide. *Nat. Chem.* **2020**, *12*, 445–451. [[CrossRef](#)] [[PubMed](#)]
6. Selkoe, D.J.; Hardy, J. The amyloid hypothesis of Alzheimer's disease at 25 years. *EMBO Mol. Med.* **2016**, *8*, 595–608. [[CrossRef](#)] [[PubMed](#)]
7. Bigi, A.; Cascella, R.; Chito, F.; Cecchi, C. Amyloid fibrils act as a reservoir of soluble oligomers, the main culprits in protein deposition diseases. *Bioessays* **2022**, *44*, e2200086. [[CrossRef](#)]
8. Tian, Y.; Viles, J.H. pH dependence of amyloid- β fibril assembly kinetics: Unravelling the microscopic molecular processes. *Angew. Chem. Int. Ed. Engl.* **2022**, *61*, e202210675. [[CrossRef](#)]
9. Thacker, D.; Willas, A.; Dear, A.J.; Linse, S. Role of hydrophobicity at the N-terminal region of A β 42 in secondary nucleation. *ACS Chem. Neurosci.* **2022**, *13*, 3477–3487. [[CrossRef](#)]
10. Nguyen, P.H.; Derreumaux, P. Insights into the mixture of A β 24 and A β 42 peptides from atomistic simulations. *J. Phys. Chem. B* **2022**, *126*, 10689–10696. [[CrossRef](#)]
11. Popov, K.I.; Makepeace, K.A.T.; Petrotchenko, E.V.; Dokholyan, N.V.; Borchers, C.H. Insight into the structure of the “unstructured” tau protein. *Structure* **2019**, *27*, 1710–1715.e4. [[CrossRef](#)] [[PubMed](#)]
12. Stelzl, L.S.; Pietrek, L.M.; Holla, A.; Oroz, J.; Sikora, M.; Köfinger, J.; Schuler, B.; Zweckstetter, M.; Hummer, G. Global structure of the intrinsically disordered protein tau emerges from its local structure. *JACS Au* **2022**, *2*, 673–686. [[CrossRef](#)]
13. Chakraborty, D.; Straub, J.E.; Thirumalai, D. Differences in the free energies between the excited states of A β 40 and A β 42 monomers encode their aggregation propensities. *Proc. Natl. Acad. Sci. USA* **2020**, *117*, 19926–19937. [[CrossRef](#)] [[PubMed](#)]
14. Santuz, H.; Nguyen, P.H.; Sterpone, F.; Derreumaux, P. Small Oligomers of A β 42 Protein in the bulk solution with AlphaFold2. *ACS Chem. Neurosci.* **2022**, *13*, 711–713. [[CrossRef](#)] [[PubMed](#)]
15. Nguyen, P.H.; Sterpone, F.; Derreumaux, P. Self-assembly of amyloid-beta (A β) peptides from solution to near in vivo conditions. *J. Phys. Chem. B* **2022**, *126*, 10317–10326. [[CrossRef](#)] [[PubMed](#)]
16. Jucker, M.; Walker, L.C. Self-propagation of pathogenic protein aggregates in neurodegenerative diseases. *Nature* **2013**, *501*, 45–51. [[CrossRef](#)] [[PubMed](#)]
17. Biasetti 2020; Al-Hilaly, Y.K.; Foster, B.E.; Biasetti, L.; Lutter, L.; Pollack, S.J.; Rickard, J.E.; Storey, J.M.D.; Harrington, C.R.; Xue, W.F.; et al. Tau (297–391) forms filaments that structurally mimic the core of paired helical filaments in Alzheimer's disease brain. *FEBS Lett.* **2020**, *594*, 944–950. [[CrossRef](#)]
18. Maina, M.B.; Al-Hilaly, Y.K.; Oakley, S.; Burra, G.; Khanom, T.; Biasetti, L.; Mengham, K.; Marshall, K.; Harrington, C.R.; Wischik, C.M.; et al. Dityrosine cross-links are present in Alzheimer's disease-derived tau oligomers and paired helical filaments (PHF) which promote the stability of the PHF-core tau (297–391) in vitro. *J. Mol. Biol.* **2022**, *434*, 167785. [[CrossRef](#)]
19. Banerjee, S.; Hashemi, M.; Zagorski, K.; Lyubchenko, Y.L. Interaction of A β 42 with membranes triggers the self-assembly into oligomers. *Int. J. Mol. Sci.* **2020**, *21*, 1129. [[CrossRef](#)]
20. Habchi, J.; Chia, S.; Galvagnion, C.; Michaels, T.C.T.; Bellaiche, M.M.J.; Ruggeri, F.S.; Sanguanini, M.; Idini, I.; Kumita, J.R.; Sparr, E.; et al. Cholesterol catalyses A β 42 aggregation through a heterogeneous nucleation pathway in the presence of lipid membranes. *Nat. Chem.* **2018**, *10*, 673–683. [[CrossRef](#)]
21. Petersen, R.B.; Peng, A. Probing the interactions between amyloidogenic proteins and bio-membranes. *Biophys. Chem.* **2023**, *296*, 106984.
22. Viles, J.H. Imaging amyloid- β membrane interactions; ion-channel pores and lipid-bilayer permeability in Alzheimer's disease. *Angew. Chem. Int. Ed. Engl.* **2023**, *62*, e202215785. [[CrossRef](#)] [[PubMed](#)]
23. Ciudad, S.; Puig, E.; Botzanowski, T.; Meigooni, M.; Arango, A.S.; Do, J.; Mayzel, M.; Bayoumi, M.; Chaignepain, S.; Maglia, G.; et al. A β (1–42) tetramer and octamer structures reveal edge conductivity pores as a mechanism for membrane damage. *Nat. Commun.* **2020**, *11*, 3014. [[CrossRef](#)] [[PubMed](#)]

24. Tian, Y.; Liang, R.; Kumar, A.; Szwedziak, P.; Viles, J.H. 3D-visualization of amyloid- β oligomer interactions with lipid membranes by cryo-electron tomography. *Chem. Sci.* **2021**, *12*, 6896–6907. [[CrossRef](#)] [[PubMed](#)]
25. Flagmeier, P.; De, S.; Michaels, T.C.T.; Yang, X.; Dear, A.J.; Emanuelsson, C.; Vendruscolo, M.; Linse, S.; Klenerman, D.; Knowles, T.P.J.; et al. Direct measurement of lipid membrane disruption connects kinetics and toxicity of A β 42 aggregation. *Nat. Struct. Mol. Biol.* **2020**, *27*, 886–891. [[CrossRef](#)] [[PubMed](#)]
26. Saha, J.; Bose, P.; Dhakal, S.; Ghosh, P.; Rangachari, V. Ganglioside-enriched phospholipid vesicles induce cooperative A β oligomerization and membrane disruption. *Biochemistry* **2022**, *61*, 2206–2220. [[CrossRef](#)] [[PubMed](#)]
27. Rana, M.; Sharma, A.K. Cu and Zn interactions with A β peptides: Consequence of coordination on aggregation and formation of neurotoxic soluble A β oligomers. *Metallomics* **2019**, *11*, 64–84. [[CrossRef](#)] [[PubMed](#)]
28. Budvytyte, R.; Valincius, G. The interactions of amyloid β aggregates with phospholipid membranes and the implications for neurodegeneration. *Biochem. Soc. Trans.* **2023**, *51*, 147–159. [[CrossRef](#)] [[PubMed](#)]
29. Zhu, X.; Liu, W.; Zhao, W.; Chang, Z.; Yang, J. The co-effect of copper and lipid vesicles on A β aggregation. *Biochim. Biophys. Acta Biomembr.* **2023**, *1865*, 184082. [[CrossRef](#)]
30. Zhu, M.; Zeng, L.; Li, Z.; Wang, C.; Wu, L.; Jiang, X. Revealing the nanoarchitectonics of amyloid β -aggregation on two-dimensional biomimetic membranes by surface-enhanced infrared absorption spectroscopy. *ChemistryOpen* **2023**, *12*, e202200253. [[CrossRef](#)]
31. Kenyaga, J.M.; Cheng, Q.; Qiang, W. Early stage β -amyloid-membrane interactions modulate lipid dynamics and influence structural interfaces and fibrillation. *J. Biol. Chem.* **2022**, *298*, 102491. [[CrossRef](#)] [[PubMed](#)]
32. Feuillie, C.; Lambert, E.; Ewald, M.; Azouz, M.; Henry, S.; Marsaudon, S.; Cullin, C.; Lecomte, S.; Molinari, M. High speed AFM and nanoinfrared spectroscopy investigation of A β _{1–42} peptide variants and their interaction with POPC/SM/Chol/GM1 model membranes. *Front. Mol. Biosci.* **2020**, *7*, 571696. [[CrossRef](#)] [[PubMed](#)]
33. Ida, A.; Abe, M.; Nochi, M.; Soga, C.; Unoura, K.; Nabika, H. Promoted aggregation of A β on lipid bilayers in an open flowing system. *J. Phys. Chem. Lett.* **2021**, *12*, 4453–4460. [[CrossRef](#)] [[PubMed](#)]
34. Baumann, K.N.; Šneiderienė, G.; Sanguanini, M.; Schneider, M.; Rimon, O.; González Díaz, A.; Greer, H.; Thacker, D.; Linse, S.; Knowles, T.P.J.; et al. A kinetic map of the influence of biomimetic lipid model membranes on A β ₄₂ aggregation. *ACS Chem. Neurosci.* **2023**, *14*, 323–329. [[CrossRef](#)]
35. Azouz, M.; Feuillie, C.; Lafleur, M.; Molinari, M.; Lecomte, S. Interaction of tau construct K18 with model lipid membranes. *Nanoscale Adv.* **2021**, *3*, 4244–4253. [[CrossRef](#)]
36. Sallaberry, C.A.; Voss, B.J.; Majewski, J.; Biernat, J.; Mandelkow, E.; Chi, E.Y.; Vander Zanden, C.M. Tau and membranes: Interactions that promote folding and condensation. *Front. Cell Dev. Biol.* **2021**, *9*, 725241. [[CrossRef](#)]
37. Lasagna-Reeves, C.A.; Sengupta, U.; Castillo-Carranza, D.; Gerson, J.E.; Guerrero-Munoz, M.; Troncoso, J.C.; Jackson, G.R.; Kaye, R. The formation of tau pore-like structures is prevalent and cell specific: Possible implications for the disease phenotypes. *Acta Neuropathol. Commun.* **2014**, *2*, 56. [[CrossRef](#)]
38. Ait-Bouziad, N.; Lv, G.; Mahul-Mellier, A.L.; Xiao, S.; Zorludemir, G.; Eliezer, D.; Walz, T.; Lashuel, H.A. Discovery and characterization of stable and toxic Tau/phospholipid oligomeric complexes. *Nat. Commun.* **2017**, *8*, 1678. [[CrossRef](#)]
39. Yao, Q.Q.; Wen, J.; Perrett, S.; Wu, S. Distinct lipid membrane-mediated pathways of Tau assembly revealed by single-molecule analysis. *Nanoscale* **2022**, *14*, 4604–4613. [[CrossRef](#)]
40. Fatafta, H.; Kav, B.; Bundschuh, B.F.; Loschwitz, J.; Strodel, B. Disorder-to-order transition of the amyloid- β peptide upon lipid binding. *Biophys. Chem.* **2022**, *280*, 106700. [[CrossRef](#)]
41. Ahyayauch, H.; García-Arribas, A.B.; Masserini, M.E.; Pantano, S.; Goñi, F.M.; Alonso, A. β -Amyloid (1–42) peptide adsorbs but does not insert into ganglioside-containing phospholipid membranes in the liquid-disordered state: Modelling and experimental studies. *Int. J. Biol. Macromol.* **2020**, *164*, 2651–2658. [[CrossRef](#)] [[PubMed](#)]
42. Ahyayauch, H.; Masserini, M.; Goñi, F.M.; Alonso, A. The interaction of A β 42 peptide in monomer, oligomer or fibril forms with sphingomyelin/cholesterol/ganglioside bilayers. *Int. J. Biol. Macromol.* **2021**, *168*, 611–619. [[CrossRef](#)] [[PubMed](#)]
43. Fatafta, H.; Poojari, C.; Sayyed-Ahmad, A.; Strodel, B.; Owen, M.C. Role of oxidized Gly25, Gly29, and Gly33 residues on the interactions of A β _{1–42} with lipid membranes. *ACS Chem. Neurosci.* **2020**, *11*, 535–548. [[CrossRef](#)] [[PubMed](#)]
44. Boopathi, S.; Garduño-Juárez, R. Calcium inhibits penetration of Alzheimer’s A β _{1–42} monomers into the membrane. *Proteins* **2022**, *90*, 2124–2143. [[CrossRef](#)] [[PubMed](#)]
45. Drabik, D.; Chodaczek, G.; Kraszewski, S. Effect of amyloid- β monomers on lipid membrane mechanical parameters-potential implications for mechanically driven neurodegeneration in Alzheimer’s disease. *Int. J. Mol. Sci.* **2020**, *22*, 18. [[CrossRef](#)] [[PubMed](#)]
46. Tempra, C.; La Rosa, C.; Lolicato, F. The role of alpha-helix on the structure-targeting drug design of amyloidogenic proteins. *Chem. Phys. Lipids.* **2021**, *236*, 105061. [[CrossRef](#)] [[PubMed](#)]
47. Cholko, T.; Barnum, J.; Chang, C.A. Amyloid- β (A β 42) peptide aggregation rate and mechanism on surfaces with widely varied properties: Insights from Brownian dynamics simulations. *J. Phys. Chem. B* **2020**, *124*, 5549–5558. [[CrossRef](#)] [[PubMed](#)]
48. Fatafta, H.; Khaled, M.; Owen, M.C.; Sayyed-Ahmad, A.; Strodel, B. Amyloid- β peptide dimers undergo a random coil to β -sheet transition in the aqueous phase but not at the neuronal membrane. *Proc. Natl. Acad. Sci. USA* **2021**, *118*, e2106210118. [[CrossRef](#)]
49. Kargar, F.; Emadi, S.; Fazli, H. Dimerization of A β 40 inside dipalmitoylphosphatidyl-choline bilayer and its effect on bilayer integrity: Atomistic simulation at three temperatures. *Proteins* **2020**, *88*, 1540–1552. [[CrossRef](#)]

50. Wang, B.; Guo, C. Concentration-dependent effects of cholesterol on the dimerization of Amyloid- β peptides in lipid bilayers. *ACS Chem. Neurosci.* **2022**, *13*, 2709–2718. [[CrossRef](#)]
51. Agrawal, N.; Skelton, A.A.; Parisini, E. A coarse-grained molecular dynamics investigation on spontaneous binding of A β _{1–40} fibrils with cholesterol-mixed DPPC bilayers. *Comput. Struct. Biotechnol. J.* **2023**, *21*, 2688–2695. [[CrossRef](#)] [[PubMed](#)]
52. Cheng, S.Y.; Cao, Y.; Rouzbehani, M.; Cheng, K.H. Coarse-grained MD simulations reveal beta-amyloid fibrils of various sizes bind to interfacial liquid-ordered and liquid-disordered regions in phase separated lipid rafts with diverse membrane-bound conformational states. *Biophys. Chem.* **2020**, *260*, 106355. [[CrossRef](#)] [[PubMed](#)]
53. Dias, C.L.; Jalali, S.; Yang, Y.; Cruz, L. Role of cholesterol on Binding of amyloid Fibrils to lipid bilayers. *J. Phys. Chem. B* **2020**, *124*, 3036–3042. [[CrossRef](#)] [[PubMed](#)]
54. Nguyen, H.L.; Linh, H.Q.; Krupa, P.; La Penna, G.; Li, M.S. Amyloid β dodecamer disrupts the neuronal membrane more strongly than the mature fibril: Understanding the role of oligomers in neurotoxicity. *J. Phys. Chem. B* **2022**, *126*, 3659–3672. [[CrossRef](#)] [[PubMed](#)]
55. Panchal, M.; Loeper, J.; Cossec, J.C.; Perruchini, C.; Lazar, A.; Pompon, D.; Duyckaerts, C. Enrichment of cholesterol in microdissected Alzheimer's disease senile plaques as assessed by mass spectrometry. *J. Lipid Res.* **2010**, *51*, 598–605. [[CrossRef](#)] [[PubMed](#)]
56. Cutler, R.G.; Kelly, J.; Storie, K.; Pedersen, W.A.; Tammara, A.; Hatanpaa, K.; Troncoso, J.C.; Mattson, M.P. Involvement of oxidative stress-induced abnormalities in ceramide and cholesterol metabolism in brain aging and Alzheimer's disease. *Proc. Natl. Acad. Sci. USA* **2004**, *101*, 2070–2075. [[CrossRef](#)] [[PubMed](#)]
57. Nguyen, T.H.; Nguyen, P.H.; Ngo, S.T.; Derreumaux, P. Effect of cholesterol molecules on A β _{1–42} wild-type and mutants trimers. *Molecules* **2022**, *27*, 1395. [[CrossRef](#)] [[PubMed](#)]
58. Ngo, S.T.; Nguyen, P.H.; Derreumaux, P. Cholesterol molecules alter the energy landscape of small A β _{1–42} Oligomers. *J. Phys. Chem. B* **2021**, *125*, 2299–2307. [[CrossRef](#)]
59. Hashemi, M.; Banerjee, S.; Lyubchenko, Y.L. Free cholesterol accelerates A β self-assembly on membranes at physiological concentration. *Int. J. Mol. Sci.* **2022**, *23*, 2803. [[CrossRef](#)]
60. Chakravorty, A.; McCalpin, S.D.; Sahoo, B.R.; Ramamoorthy, A.; Brooks, C.L. 3rd. Free gangliosides can alter amyloid- β aggregation. *J. Phys. Chem. Lett.* **2022**, *13*, 9303–9308. [[CrossRef](#)]
61. Khatua, P.; Jana, A.K.; Hansmann, U.H.E. Effect of lauric acid on the stability of A β ₄₂ oligomers. *ACS Omega* **2021**, *6*, 5795–5804. [[CrossRef](#)] [[PubMed](#)]
62. Andrews, B.; Ruggiero, T.; Urbanc, B. How do salt and lipids affect conformational dynamics of A β ₄₂ monomers in water? *Phys. Chem. Chem. Phys.* **2023**, *25*, 2566–2583. [[CrossRef](#)] [[PubMed](#)]
63. Österlund, N.; Moons, R.; Ilag, L.L.; Sobott, F.; Gräslund, A. Native ion mobility-mass spectrometry reveals the formation of β -barrel shaped amyloid- β hexamers in a membrane-mimicking environment. *J. Am. Chem. Soc.* **2019**, *141*, 10440–10450. [[CrossRef](#)] [[PubMed](#)]
64. Quist, A.; Doudevski, I.; Lin, H.; Azimova, R.; Ng, D.; Frangione, B.; Kagan, B.; Ghiso, J.; Lal, R. Amyloid ion channels: A common structural link for protein-misfolding disease. *Proc. Natl. Acad. Sci. USA* **2005**, *102*, 10427–10432. [[CrossRef](#)] [[PubMed](#)]
65. Ngo, S.T.; Nguyen, P.H.; Derreumaux, P. Impact of A2T and D23N mutations on tetrameric A β ₄₂ barrel within a dipalmitoylphosphatidylcholine lipid bilayer membrane by replica exchange molecular dynamics. *J. Phys. Chem. B* **2020**, *124*, 1175–1182. [[CrossRef](#)] [[PubMed](#)]
66. Durell, S.R.; Kayed, R.; Guy, H.R. The amyloid concentric β -barrel hypothesis: Models of amyloid beta 42 oligomers and annular protofibrils. *Proteins* **2022**, *90*, 1190–1209. [[CrossRef](#)] [[PubMed](#)]
67. Sepehri, A.; Lazaridis, T. Putative structures of membrane-embedded amyloid β oligomers. *ACS Chem. Neurosci.* **2023**, *14*, 99–110. [[CrossRef](#)] [[PubMed](#)]
68. Matthes, D.; de Groot, B.L. Molecular dynamics simulations reveal the importance of amyloid-beta oligomer β -sheet edge conformations in membrane permeabilization. *J. Biol. Chem.* **2023**, *299*, 103034. [[CrossRef](#)]
69. Rando, C.; Grasso, G.; Sarkar, D.; Sciacca, M.F.M.; Cucci, L.M.; Cosentino, A.; Forte, G.; Pannuzzo, M.; Satriano, C.; Bhunia, A.; et al. GxxxG motif stabilize ion-channel like pores through C α -H \cdots O interaction in A β (1–40). *Int. J. Mol. Sci.* **2023**, *24*, 2192. [[CrossRef](#)]
70. Nguyen, P.H.; Derreumaux, P. An S-shaped A β ₄₂ cross- β hexamer embedded into a lipid bilayer reveals membrane disruption and permeability. *ACS Chem. Neurosci.* **2023**, *14*, 936–946. [[CrossRef](#)]
71. Press-Sandler, O.; Miller, Y. Molecular insights into the primary nucleation of polymorphic amyloid β dimers in DOPC lipid bilayer membrane. *Protein Sci.* **2022**, *31*, e4283. [[CrossRef](#)]
72. MacAinsh, M.; Zhou, H.X. Partial mimicry of the microtubule binding of tau by its membrane binding. *Protein Sci.* **2023**, *32*, e4581. [[CrossRef](#)] [[PubMed](#)]
73. Georgieva, E.R.; Xiao, S.; Borbat, P.P.; Freed, J.H.; Eliezer, D. Tau binds to lipid membrane surfaces via short amphipathic helices located in its microtubule-binding repeats. *Biophys. J.* **2014**, *107*, 1441–1452. [[CrossRef](#)] [[PubMed](#)]
74. Brotzakis, Z.F.; Lindstedt, P.R.; Taylor, R.J.; Rinauro, D.J.; Gallagher, N.C.T.; Bernardes, G.J.L.; Vendruscolo, M. A structural ensemble of a tau-microtubule complex reveals regulatory tau phosphorylation and acetylation mechanisms. *ACS Cent. Sci.* **2021**, *7*, 1986–1995. [[CrossRef](#)] [[PubMed](#)]

75. Nguyen, P.H.; Derreumaux, P. Molecular dynamics simulations of the tau R3-R4 domain monomer in the bulk Solution and at the surface of a lipid bilayer model. *J. Phys. Chem. B* **2022**, *126*, 3431–3438. [[CrossRef](#)] [[PubMed](#)]
76. Takeda, S.; Commins, C.; DeVos, S.L.; Nobuhara, C.K.; Wegmann, S.; Roe, A.D.; Costantino, I.; Fan, Z.; Nicholls, S.B.; Sherman, A.E.; et al. Seed-competent high-molecular-weight tau species accumulates in the cerebrospinal fluid of Alzheimer’s disease mouse model and human patients. *Ann. Neurol.* **2016**, *80*, 355–367. [[CrossRef](#)] [[PubMed](#)]
77. Nguyen, P.H.; Derreumaux, P. Molecular dynamics simulations of the tau amyloid fibril core dimer at the surface of a lipid bilayer model: I. In *Alzheimer’s disease*. *J. Phys. Chem. B* **2022**, *126*, 4849–4856. [[CrossRef](#)] [[PubMed](#)]
78. Cheng, K.H.; Graf, A.; Lewis, A.; Pham, T.; Acharya, A. Exploring membrane binding targets of disordered human tau aggregates on lipid rafts using multiscale molecular dynamics simulations. *Membranes* **2022**, *12*, 1098. [[CrossRef](#)] [[PubMed](#)]
79. Chowdhury, U.D.; Paul, A.; Bhargava, B.L. The effect of lipid composition on the dynamics of tau fibrils. *Proteins* **2022**, *90*, 2103–2115. [[CrossRef](#)]

Disclaimer/Publisher’s Note: The statements, opinions and data contained in all publications are solely those of the individual author(s) and contributor(s) and not of MDPI and/or the editor(s). MDPI and/or the editor(s) disclaim responsibility for any injury to people or property resulting from any ideas, methods, instructions or products referred to in the content.